RELATING THE CHANNEL TO ACOUSTIC MODEM PERFORMANCE

Michael B. Porter

Science Applications International Corporation
888 Prospect St., Suite 201, La Jolla, California, USA 92037
email: michael.b.porter@saic.com

Vincent K. McDonald, Paul A. Baxley and Joseph A. Rice

Space and Naval Warfare Systems Center, San Diego
49575 Gate Road, San Diego, California, USA 92152-6435
email: vmcdonal, baxley, rice @spawar.navy.mil

The potential of undersea acoustic modems has become increasingly obvious in recent years leading to a significant research and development program. In the near future, such modems will likely form the link between surface and submerged platforms; connect undersea surveillance systems; and link ocean-bottom seismometers to the surface to name just a few of the many applications. One would like to squeeze the best performance out of such modems in terms of energy usage (battery life), data rate, and manufacturing cost. They should also be robust in their ability to function in different acoustic environments and in the presence of strong interferers. A variety of signalling schemes have been proposed, however, the performance of such schemes in relation to the environment is not well understood. To address this issue, a series of experiments (SignalEx) will be conducted in diverse environments. This paper describes the lessons learned from the ModemEx pilot experiment.

1. INTRODUCTION

The SignalEx pilot experiment (ModemEx), was conducted in April 1999, 6 km southwest of San Diego. As details of this experiment have been presented elsewhere [1] we summarize this only briefly. The bathymetry and source track are shown in Fig. 1. A key component of this test was a versatile telesonar testbed [2,3] developed at the Space and Naval Warfare Systems Center. This is an autonomous unit that consists of a single-board computer with a projector and 4-phone vertical line array.
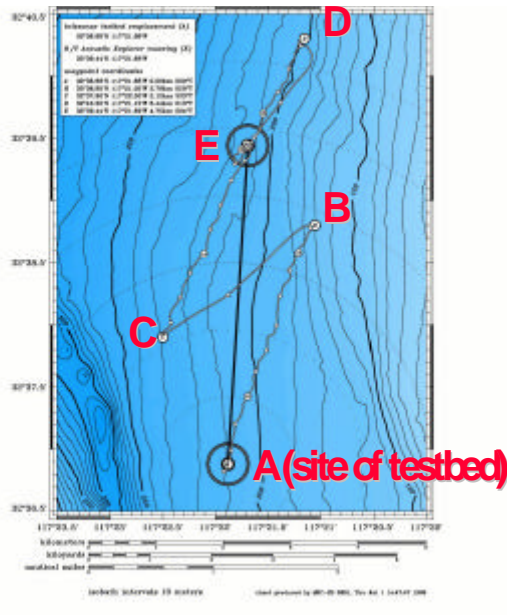
Event 3
- Drifting track A-B
- 0 to 3.8 km

Event 4
- Drifting track C-D
- 2.1 to 6.5 km

Event 5
- Stationary at E
- 4.75 km

Fig. 1: Bathymetry and source track.

The autonomous testbed was deployed on the ocean bottom at a depth of about 215 m. Meanwhile, a separate over-the-side the testbed was set up on the Acoustic Explorer research vessel with a single projector and receiver deployed over the side at a depth of about 30 m. Transmissions of both probe signals and data were transmitted in 10-minute cycles in alternating directions between the testbeds over a 5-hour period.

Northerly winds caused the ship to drift from a range of about 0 to 4 km ('First drift'). As the range was becoming large and the ship began drifting off the iso-bath, the ship was repositioned back at a range of about 2 km and allowed to drift again ('Second drift'). This conveniently provided a look at the consistency of the Phase I results. Once again the ship drifted to a range of about 6.5 km and was repositioned and moored at a range of 4.75 km providing a look at the stability of the signaling schemes with fixed source-receiver geometry.

A variety of signalling schemes were tested during the experiment and are being analysed by their various developers. Here we summarize only the performance of 'Datasonics type-a', which is a commercial multi-frequency shift keying (MFSK) system [4]. This was decoded in real-time during the course of the experiment. During most of the test, type-a signals were decoded with few errors. However, in the range of 4-4.75 km there were significant decoding problems; beyond 4.75 km, performance again became nearly perfect. In the remainder of this paper, we will try to interpret this performance variation and simultaneously illustrate that the acoustic models accurately characterize the channel physics.

2. ANALYSIS OF PROBE SIGNALS

A set of linear frequency-modulated waveforms (chirps) was sent 4 times during each 10-minute transmission to estimate the channel impulse response. The chirps swept from 8 kHz to 16 kHz over a 1-second period. Four such chirps were contained in each probe yielding a total of 16 transmissions in each 10-minute frame. In a standard process, channel impulse
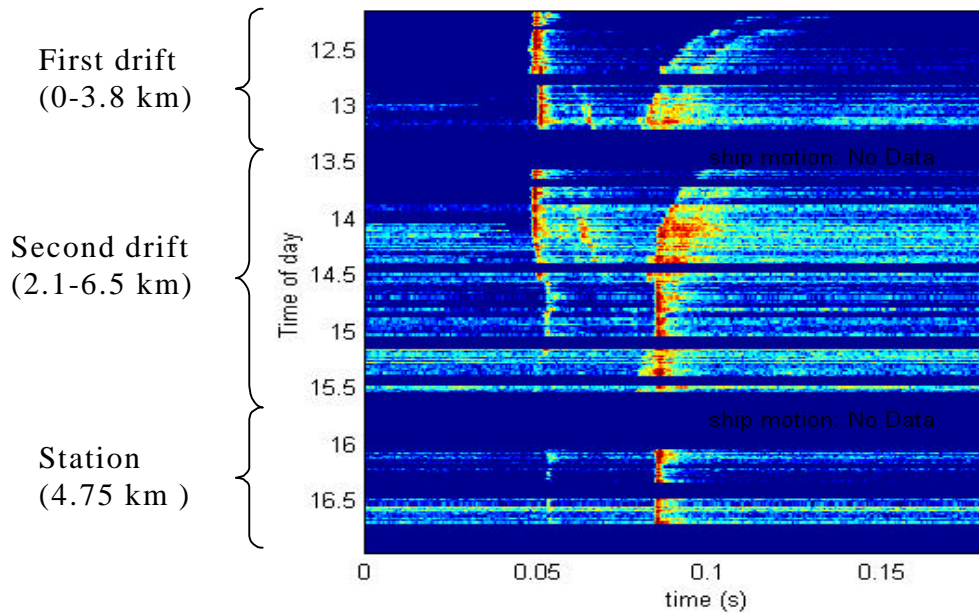
First drift
(0-3.8 km)

Second drift
(2.1-6.5 km)

Station
(4.75 km)

Fig. 2: Replica correlogram from chirps.

response is then estimated by correlating the received waveform with a replica of the transmitted waveform. This produces a sequence of impulses corresponding to each echo in the received waveform thereby providing a visualization of the impulse response. The result is shown in Fig. 2 and shows clearly the variation in the multipath structure throughout the experiment. Since absolute times were not available, the first significant peak in each reception was detected and used to provide a leading-edge alignment. Note also that this plot is a composite of the transmissions that alternated between the ship and bottom-mounted testbeds.

3. ACOUSTIC MODELING

The sound-speed profile is shown in Fig. 3. The ocean bottom was modeled as a half-space with sound speed of 1572 m/s, density of 1.5 gm/cm^3, and attenuation of 0.2 dB/wavelength. These values are based on extensive experience in the area with matched-field tracking for SwellEx [5].

To interpret the arrival structure in the replica correlogram we begin with a ray/beam [6, 7] calculation also shown in Fig. 3. Transmission loss was calculated using the carrier frequency of 12 kHz and using an incoherent option that discards the phase associated with each ray. The superimposed ray-trace shows the correspondence between the field intensity and the rays contributing at a give location.

There are two classes of rays. The first set, shown in blue, consists of refracted/bottom-reflected (RBR) paths (i.e. paths that do not hit the surface). The second set, shown in green, consists of surface-reflected/bottom-reflected (SRBR) paths that interact with both boundaries. The strength of these various paths is sometimes difficult to estimate; however, we can anticipate that a fairly strong arrival will be seen in the region out to 2.3 km where
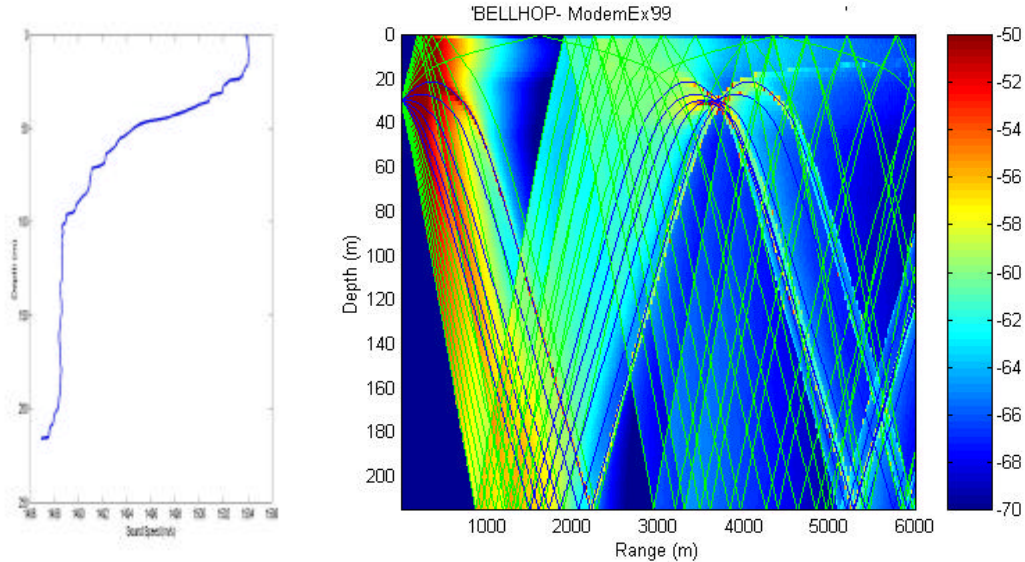
Fig. 3: Sound-speed profile and ray trace.

there is a direct path from the source to the testbed receiver near the bottom. Beyond that range, the contributing paths reflect off one or both of the boundaries where they will experience a loss due to scatter. At a range of about 5 km we see the RBR rays coming in with a fairly tight spread; since the ray-tube cross-section is a measure of the intensity, we make expect an improvement in signal level there.

It is also useful to look at the eigenray picture obtained by taking a fixed receiver position and identifying the rays in Fig. 3 that pass through (or near) that receiver. In Fig. 4 we show the eigenrays for a source-receiver separation of 2.5 km (left panel) and 5 km (right panel). Looking first at the left panel, we see in order of their expected arrival time, a direct path (black); a refracted/bottom-reflected path (blue); a surface reflected path (red) and a surface-reflected/bottom-reflected path (green). Turning to the right panel, we see that there are now several additional paths corresponding to higher-order surface and bottom reflections.

Next we consider the predicted impulse response as a function of source-receiver separation. Here the fan of ray take-off angles has been expanded to +/- 40 degrees to capture the steeper angle paths. The horizontal axis shows reduced time, meaning the time relative to a window that pans with the pulse at a speed of 1500 m/s. A sinc pulse was used with an 8-kHz central frequency and the log of the envelope is shown in Fig. 5 using a source of arbitrary amplitude.

Using our knowledge of the ray paths gained from the previous plots, we can now readily identify the features in this plot. In the very near field (ranges less than 500 m) we see just four arrivals. These are the direct (D), bottom bounce (B), surface bounce (S), and surface-bottom bounce (SB). Note that the bottom-bounce path follows a trajectory almost identical to the direct except that it must go a small extra distance to hit the bottom and come back to the receiver. Since the testbed receivers are about 6 m above the seafloor, the D and B arrivals are almost indistinguishable in time with this source pulse.

Similarly the surface bounce must travel the extra distance to the surface and back. The ship source is located some 30 m below the sea surface so the S arrival comes some 20 msecs after D and B. The SB path makes a short extra trip to the bottom and arrives at almost the same time as the S path.
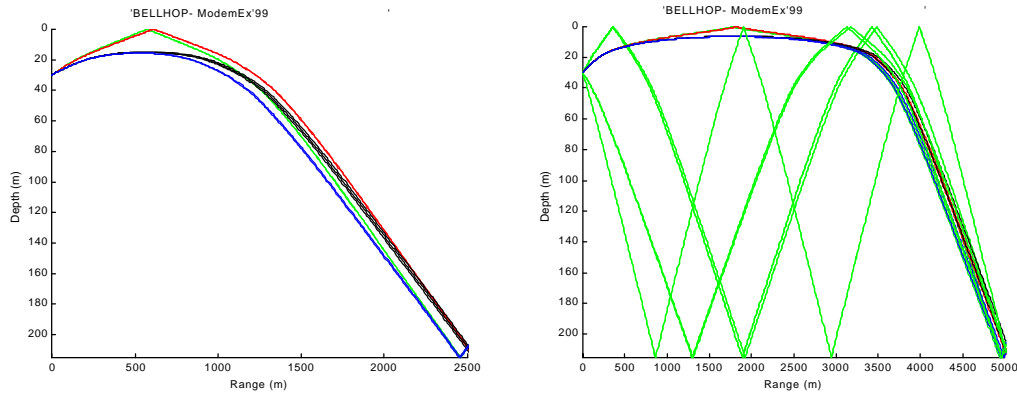
Fig. 4: Eigenrays for the testbed at 2.5 km range (left) and 5 km range (right).

At a source/receiver separation of about 700 m, we start to see higher order surface and bottom bounce paths coming in. At about 3000 m, the D, B, S, and SB have essentially vanished (as may be seen in Fig. 3), but still higher-order paths are starting to come in. At about 5000 m we start to see a quite strong arrival as a new set of paths (again visible in Fig. 3) starts to come in.

The model results may now be used to interpret the replica correlogram keeping in mind that it was aligned by a leading edge associated with the first arrival. To make the correspondence we also need to be aware of the variation in range during each of the phases of the experiment. The first drift covered a range of about 2 to 5 km and we see a good correspondence with the modelled arrival structure covering that set or ranges. The second drift traces out that same pattern again but this time goes to a greater range where the strong arrival seen at about 5000 m in the simulation starts to dominate.

4. CONCLUSIONS

Acoustic modem performance can be strongly influenced by the environment. More significantly, these effects can be understood and even predicted with modern acoustic channel models. We have seen in some environments and at lower frequencies that the multipath structure is dominated by a sequence of surface and bottom reflections, with the overall duration increasing systematically with range. However, the communications frequencies used in ModemEx are significantly higher than those typically used for surveillance. In addition, the ocean bottom is softer. These two features lead to an impulse response dominated by a few, strongly refracted paths with complicated transitions in range. In particular, in the 4-4.75 km range there are no strong paths but at approximately 5 km a new set of energetic paths comes in. This transition explains the communications drop out and subsequent re-acquisition experienced during ModemEx.

The propagation conditions can vary significantly with the test site with associated strong variations in modem performance. For instance, in other work with upward refracting conditions, we have seen significantly shorter communications ranges with error rates clearly driven by the variation in wind speed. The continuing SignalEx tests will provide confidence in the predictive capability of the models and ultimately lead to improved modem designs.
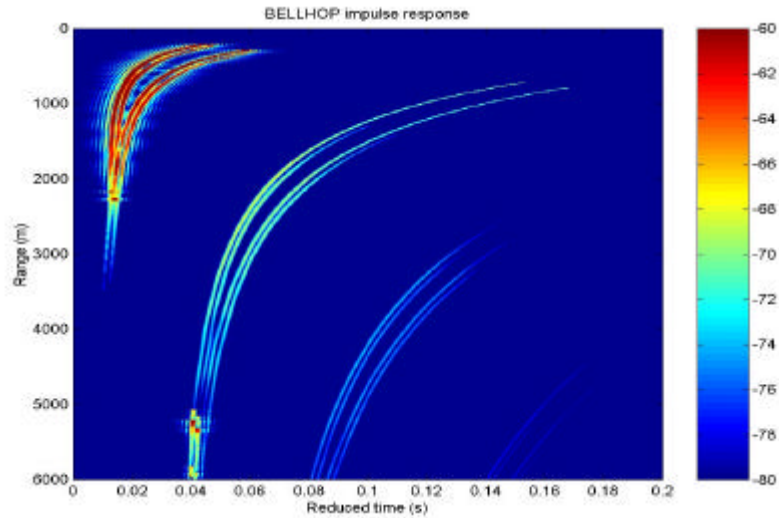
Fig. 5: Ray/beam simulation of the channel impulse response.

5. ACKNOWLEDGEMENTS

REFERENCE

[1] V. K. McDonald, J.A. Rice, Michael B. Porter, Paul A. Baxley, "Performance measurements of a diverse collection of undersea, acoustic, communication signals", *Proc. I.E.E.E. Oceans'99*, Seattle, Washington (1999).

[2] V. K. McDonald, J. A. Rice, "Telesonar testbed -- advances undersea wireless communication," *Sea Technology*, Vol. 40(2), pp. 17-23, 1999.

[3] V.K. McDonald, J.A. Rice, and C.L. Fletcher, "An underwater communication testbed for Telesonar RDT&E," *Ocean Community Conference '98, The Marine Technology Society Annual Conference*, Baltimore, Nov. 16-19, 1998.

[4] K.E. Scussel, J.A. Rice, and S. Merriam, "A new MFSK acoustic modem for operation in adverse underwater channels," *Proc. IEEE Oceans'97*, Halifax, Nova Scotia, pp. 247-254, 1997.

[5] Paul A. Baxley, Newell O. Booth, and William S. Hodgkiss, "Matched-field replica model optimisation and bottom property inversion in shallow water," *J. Acoust. Soc. Amer.*, Vol. 107(3), pp. 1301-1323, 2000.

[6] Paul A. Baxley, Homer Bucker, and Joseph A. Rice, "Shallow-water acoustic communications channel modeling using three-dimensional Gaussian beams," Ocean Community Conference '98, Baltimore, Nov. 16-19, 1998.

[7] F. Jensen, W. Kuperman, M. Porter and H. Schmidt, *Computational Ocean Acoustics*, Springer-Verlag (2000).